Monthly and seasonal streamflow forecasting of large dryland catchments in Brazil

Alexandre C COSTA[1*], Alvson B S ESTACIO[2], Francisco de A de SOUZA FILHO[2], Iran E LIMA NETO[2]

[1] Institute of Engineering and Sustainable Development, University of International Integration of the Afro-Brazilian Lusophony, Redenção, CEP 62.790-970, Brazil;
[2] Department of Hydraulic Engineering and Environment, Federal University of Ceará, Fortaleza, CEP 60.451-970, Brazil

Abstract: Streamflow forecasting in drylands is challenging. Data is scarce, catchments are highly human-modified and streamflow exhibits strong nonlinear responses to rainfall. The goal of this study was to evaluate the monthly and seasonal streamflow forecasting in two large catchments in the Jaguaribe River Basin in the Brazilian semi-arid area. We adopted four different lead times: one month ahead for monthly scale and two, three and four months ahead for seasonal scale. The gaps of the historic streamflow series were filled up by using rainfall-runoff modelling. Then, time series model techniques were applied, i.e., the locally constant, the locally averaged, the k-nearest-neighbours algorithm (k-NN) and the autoregressive model (AR). The criterion of reliability of the validation results is that the forecast is more skillful than streamflow climatology. Our approach outperformed the streamflow climatology for all monthly streamflows. On average, the former was 25% better than the latter. The seasonal streamflow forecasting (SSF) was also reliable (on average, 20% better than the climatology), failing slightly only for the high flow season of one catchment (6% worse than the climatology). Considering an uncertainty envelope (probabilistic forecasting), which was considerably narrower than the data standard deviation, the streamflow forecasting performance increased by about 50% at both scales. The forecast errors were mainly driven by the streamflow intra-seasonality at monthly scale, while they were by the forecast lead time at seasonal scale. The best-fit and worst-fit time series model were the k-NN approach and the AR model, respectively. The rainfall-runoff modelling outputs played an important role in improving streamflow forecasting for one streamgauge that showed 35% of data gaps. The developed data-driven approach is mathematical and computationally very simple, demands few resources to accomplish its operational implementation and is applicable to other dryland watersheds. Our findings may be part of drought forecasting systems and potentially help allocating water months in advance. Moreover, the developed strategy can serve as a baseline for more complex streamflow forecast systems.

Keywords: nonlinear time series analysis; probabilistic streamflow forecasting; reconstructed streamflow data; dryland hydrology; rainfall-runoff modelling; stochastic dynamical systems

1 Introduction

Brazil is a land where water abounds. However, this resource is unevenly distributed throughout the

*Corresponding author: Alexandre C COSTA (E-mail: cunhacos@unilab.edu.br)
Received 2020-10-27; revised 2021-02-17; accepted 2021-02-20

country's territory. A particularly drought-prone region is the northeast part of the country, which has been struck by over 100 severe droughts since the 16th century (Fioreze et al., 2012). A period of exceptionally strong droughts is currently affecting the region since 2012 with severe social and economic consequences. Despite the extreme environmental conditions, more than 25% of the Brazilian population live within the so-called "drought polygon" in northeastern Brazil (NE-Brazil) (Formiga-Johnsson and Kemper, 2005).

Water management and planning in NE-Brazil has been centered on the storage of surface water by building dams (Araújo, 1990). In the drought polygon, groundwater resources are generally scarce, and so several thousands of reservoirs (mostly small dams) have been built in recent decades. An interstate water transfer system is also under construction (Nunes, 2012). In the last 30 a, the creation of sub-basin committees and user commissions has involved hundreds of stakeholders such as municipalities, public and large private irrigators, fishermen and industry leaders in the process of water allocation and conflict resolution. These experiences were very important transformations in water management practices and increased the demands for technical support, principally in the form of streamflow forecasts, which perfectly fall within a context of proactive drought risk management (Crochemore et al., 2016).

Reliable seasonal streamflow forecast information is a key aspect of drought mitigation (Shukla and Lettenmaier, 2011), since the water allocation process for a given rainy season may start prior to its end, optimizing water releases to multiple competing users. Also, measures of water demand reduction can be applied more efficiently, avoiding abrupt water shortages. Despite the widespread recognition of the relevance and importance of seasonal streamflow forecasting (SSF) in the research community, forecasting of streamflow for drought management has not been applied widely (Trambauer et al., 2015). The forecast information must satisfy the need for a thorough drought assessment without overwhelming end users with high complexity (Seibert et al., 2017).

Approaches for SSF predominantly fall into two categories: statistical or dynamic. The former frequently utilizes predictors of sea-surface temperature or a related index to directly estimate streamflow through regression techniques (Seibert et al., 2017; Delgado et al., 2018). The latter seeks to use numerical climate models linked with conceptual or physically based hydrological models through either an iterative (online) or static (offline) procedure strategy (Collischonn et al., 2007; Yossef et al., 2013; Yuan, 2016; Yuan et al., 2016).

Souza Filho and Lall (2003) developed a semiparametric approach for forecasting inflows at reservoirs in the State of Ceará (Ceará) in NE-Brazil conditional on the NINO3 (the mean monthly temperature anomaly in the area of the eastern tropical pacific: 5S-5N; 150W–90W) index for the El Niño Southern Oscillation (ENSO) and an equatorial Atlantic sea surface temperature index. Forecasts of January through December streamflow were made at three lead times: in January of the same year and in October and July of the preceding year. Large-scale climatic patterns have commonly been applied for improving long lead time streamflow forecasts (Moradkhani and Meier, 2010; Kalra et al., 2012; Kalra et al., 2013). They found the streamflow at the Ceará sites is highly spatially correlated and is influenced by climate in a similar manner, leading to a common, underlying model for all sites. Although the correlation of the median forecast with the observed annual inflows of Orós reservoir, the second largest reservoir in Ceará, was consistently high (0.91) for the validation period (1993–2000), the dispersion of the forecasting ensemble was quite high too, reaching, for example, 65% of the reservoir capacity (difference between 75th and 25th percentiles of ensemble forecasts) in 2000.

Delgado et al. (2018) assessed a set of seasonal drought forecast models for the Jaguaribe River in semi-arid NE-Brazil. The forecast issue time was January and the forecast period was January to June. Their work employed a cascade of models and algorithms ranging from two general circulation models (GCM) (one atmospheric and one coupled) at the top to hydrological indices at the bottom. Three statistical, meteorological downscaling approaches were applied to the GCM outputs. Reservoir volumes were obtained by fitting a multivariate linear regression based on forecast meteorological drought indices as predictors, such as Standardized Precipitation Index (SPI) and Standardized Precipitation Evapotranspiration Index (SPEI) at different timescales. They found that low precipitation events showed either very low or no skill. Moreover, the good skill of the reservoir

storage forecast was likely related to the long memory of the reservoir system, because the forecasted precipitation will affect the reservoir only marginally, since most of its storage is accumulated throughout several years. In fact, no approach had a Root Mean Square Error (RMSE) that significantly departed from the RMSE of the climatology (Delgado et al., 2018), i.e., the observed long-term average of a variable.

Pilz et al. (2019) evaluated and compared the performances of seasonal reservoir storage forecasts derived by a process-based, semi-distributed hydrological model and a statistical approach, which was developed by Delgado et al. (2018). They found, in a hindcast experiment (1981–2014), the accuracy of estimating regional reservoir storages was considerably lower using the hydrological model. In fact, investigations regarding the deficiencies of the process-based model revealed a significant influence of antecedent wetness conditions and a higher sensitivity of model prediction performance to rainfall forecast quality.

Applying a framework of GCM, multiple regional climate models, including dynamical and statistical models, and two lumped water balance models, Block et al. (2009) produced ensemble streamflow forecasts for a hindcast of 1974–1996 monthly streamflow of the Jaguaribe River. The best coupled model demonstrated high skill scores for the correlation (0.90) and the RMSE (8.1×10^7 m^3) (based on the ensemble median), but performed inferiorly to climatology for the ranked probability skill score (Wilks, 2005). Afterwards, Kwon et al. (2012) showed the uncertainties associated with the climate forecast are much larger than those from parameter estimation in the assumed hydrological model. So, the past studies pointed out no dynamical, statistical or hybrid approach outperformed the climatology for the streamflow forecasting in the Jaguaribe River Basin.

Poor or lower performance of forecasting systems for (very) dry catchments has also been reported by other authors. Robertson and Wang (2012) introduced a predictor selection method for a Bayesian joint probability approach to 3-month-ahead streamflow forecasting at multiple sites in two catchments in eastern Australia. They found out that the skill scores were considerably lower for the intermittent rivers in the Burdekin River catchment than the perennial ones in the Goulburn River catchment. In fact, in the Burdekin River catchment, the skill of the streamflow forecasts was close to zero for many months. Sittichok et al. (2016) combined statistical rainfall forecasting models with rainfall-runoff modelling in the Sahel region. They found out moderate skill (coefficient of determination equal to 0.55) for the monthly streamflow with a 12-month forecasting lead time in the Sirba watershed, West Africa. Seibert et al. (2017) applied multiple linear models, artificial neural networks and random forest regression trees to forecast seasonal hydrological drought (standardized streamflow index) in the Limpopo River Basin in southern Africa. The models were set up to predict the standardised total streamflow of December–May, which is one value per year, at the lead times of 1, 2, 3, 6, 9 and 12 months. At some streamflow stations, skill is present up to a 12-month lead time, but many stations (larger catchments in particular) only achieved little skill. These large catchments have not only a higher degree of human interference, but also drain large drylands in the Limpopo River Basin. Bennett et al. (2017) assessed a forecasting system based on a monthly rainfall-runoff model forced by ensemble rainfall forecasts for 63 Australian catchments, including 21 ephemeral rivers. Although this system generally produced skillful forecasts at shorter lead times (<4 months), it did not perform well in very dry catchments, sometimes producing strongly negative forecast skill and poor reliability. Moreover, dry catchments are typically streamflow data-scarce environments, where the streamflow gauges are sparse, whose time series are normally short (from some years to few decades) and with a lot of gaps. Thus, overall, monthly streamflow forecasting and SSF in drylands is challenging.

Although there are only a few examples in the literature, nonlinear univariate time series models have been shown as a promising tool to forecast semi-arid streamflow at daily (He et al., 2014) and monthly scales (Yassen et al., 2016). In this study, we propose to analyze the potentiality of the streamflow series itself for streamflow forecasting at monthly to seasonal time scales in two large catchments in the Jaguaribe River Basin, using nonlinear time series analysis. The specific objectives are to fill the gaps and increase the available streamflow data and to produce deterministic and probabilistic monthly streamflow forecasting for different lead times (one-, two-, three- and four-

months-ahead). The studied semi-arid catchments have a high streamflow interannual variability and relatively short time series with several gaps. A rainfall-runoff model was used to fill up the streamflow gaps. To our knowledge, this kind of hydrological model application for dryland streamflow forecasting has not been reported yet. Moreover, due to time series shortness, the chosen time series models were kept as simple as possible.

2 Study area and streamflow data

Ceará (Fig. 1) is the home to more than eight million people. The climate is predominantly semi-arid, covering more than 90% of its territory. The mean annual precipitation is about 810 mm, ranging from more than 1200 mm close to the coast, especially in some mountainous regions, to less than 600 mm in the large semi-arid landscape that extends from the coast to the interior borders (Werner and Gerstengarbe, 2003). The actual evapotranspiration is about 78% of the annual rainfall (SUDENE, 1980) while the potential evapotranspiration is four times the annual rainfall. The rainy season is mainly concentrated from February to May, accounting for about 70% of the annual rainfall.

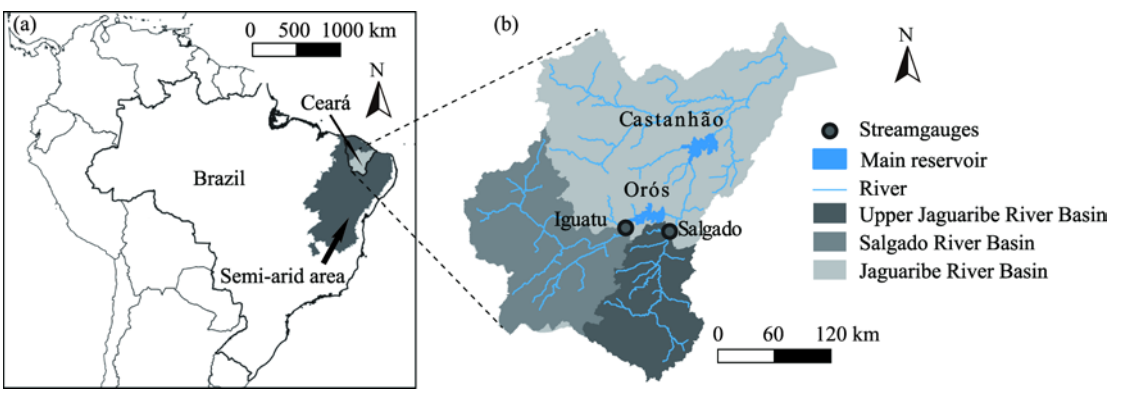

Fig. 1 Location of the Brazilian semi-arid area, the State of Ceará (Ceará) and the Jaguaribe River Basin (a), with the main reservoirs and streamgauges (b) used in this study

Interannual rainfall anomalies are driven primarily by anomalous patterns of Sea Surface Temperature (SST) variability in the Tropical Atlantic and the Equatorial Pacific (Hastenrath and Heller, 1977; Moura and Shukla; 1981, Uvo et al., 1998; Rodrigues et al., 2011). During the rainy season, the southernmost displacement of the Intertropical Convergence Zone in the Atlantic Ocean allows the enhancement of atmospheric conditions to precipitation events over or nearby Ceará. Interannual and seasonal fluctuations assigned to excess (lack) of rainfall over Ceará are associated with asymmetrical interhemispheric gradient of SST anomalies in the Tropical Atlantic oriented northward (southward) (Hastenrath and Heller, 1977; Moura and Shukla, 1981; Nobre and Shukla, 1996). Also, on interannual timescales, accumulated rainfall in Ceará is strongly modulated by the ENSO, which is the prominent interannual mode associated to coupled oceanic-atmospheric interactions in the Equatorial Pacific (Philander, 1990; Rao and Hada, 1990). The warm (cold) oceanic phase of the ENSO is known as El Niño (La Niña) that is marked by an abnormal warmer (colder) SST anomalies in the eastern-central Pacific modifying the Walker circulation and leading to unfavourable (favourable) atmospheric conditions over Ceará.

The streamflow is naturally ephemeral or intermittent. It ranges from 10% to 20% of annual rainfall and shows high temporal variability with a coefficient of variation generally above 1.00 at an interannual scale (Güntner and Bronstert, 2004). The large rivers are dominantly endogenous and interact with the underlying groundwater mainly by groundwater recharge (Costa et al., 2012a; 2013). Yet the groundwater resources are scarce and concentrated, occurring largely in sedimentary rocks on the state borders and on the coast, besides a sedimentary basin located in the middle of the state (Frischkorn et al., 2003).

The recurrent droughts have been essentially treated as a supply problem to be resolved through

massive construction and related water infrastructure, such as dams and water transfer schemes among watersheds (Gutiérrez et al., 2014). As a result, there are more than 7000 dams with a surface area larger than 5 hm^2 in Ceará (FUNCEME, 2008), which produce a dense reservoir network that highly impact the runoff connectivity at catchment scale and the river flow propagation (Güntner et al., 2004; Mamede et al., 2012). The state and federal agencies manage 155 dams, which store 18.7×10^9 m^3, providing more than 90% of the water supply in Ceará. The two largest reservoirs are the Castanhão and the Orós reservoirs with a capacity of 6.7×10^9 and 1.94×10^9 m^3, respectively (Fig. 1). The Upper Jaguaribe River and its main tributary, the Salgado River, are the principal runoff sources of the Jaguaribe River Basin. Their flows have been monitored by the Brazilian Geological Service at Salgado streamgauge (SS) and Iguatu streamgauge (IS) (Fig. 1), which drain areas of 12,400 and 20,700 km^2, respectively. This study concentrates on the river flows monitored at these streamgauges. Their daily streamflow data are made available by the Brazilian Water Agency (http://www.hidroweb.ana.gov.br). We consider a period of analysis from 1951 to 2015. Under this period, the IS shows few gaps, only 3.7% of the whole data (29 months). The gaps in the streamflow series of the SS represent 35.1% of the data (278 months).

3 Methodology

3.1 Time series models

We assumed that the streamflow series is driven by a stochastic dynamical system, which governs the coupling between the climatological forcing and the human-modified catchment state that depends on natural landscape characteristics and anthropogenic effects, such as land use changes, reservoir construction and water withdrawal (Kirchner, 2009; Sivakumar and Singh, 2012; Costa et al., 2012b). A stochastic dynamical system can be expressed mathematically by time series models. The deterministic evolution operator (the dynamical or deterministic part) is approached by the dynamics of values of a unique variable (the delay embedding theorem; Takens, 1980), whereas the stochastic part by noise, which does not depend on the states of the dynamical part (Costa et al., 2012b). In real-world open physical systems, such as catchment runoff, the presence of dynamical and data noise are inevitable (Porporato and Ridolfi, 2001; Kantz and Schreiber, 2004). Equation 1 describes a stochastic dynamical system.

$$x_{t+m\Delta t} = F\left(x_t,\ x_{t-\Delta t},\ \ldots,\ x_{t-\Delta t(n-1)}\right) + \xi, \tag{1}$$

where $x_{t+\Delta t\times m}$ is the forecast, $\Delta t\times m$ is the lead time, m is a positive natural number, F is the deterministic term, n is the number of past steps and ξ could be white and coloured noise. Considering a training set, we can empirically determine the ξ distribution by assuming a regression model to F. Note that the distribution of ξ includes the uncertainty not only from the inherent fluctuations of the streamflow data, but also from the fitting of the underlying dynamical term by an adopted regression model (Costa et al., 2012b). So, the expected value of the forecast is equal to the deterministic term F, and the uncertainty involved is calculated by the distribution of ξ with a confidence interval, e.g., 50%, ascribing in this way a probability density function (PDF) or an uncertainty envelope for $x_{t+\Delta t\cdot m}$.

We selected four regression models: (1) the locally constant (LC), whose prediction is just equal to the last streamflow measurement; (2) the locally averaged (LA), whose prediction is the average over the streamflow measurements at n last steps; (3) the traditional k-NN, whose prediction is up to the k number (ranging from 1 to 7 in this study) of neighbours and to the power parameter of the inverse distance weighting interpolation; and (4) the autoregressive model (AR), whose unknown parameters are the number of the streamflow measurements at n last steps and its coefficients. The latter was used for the dynamical term F as reference to test the hypothesis of linear random data. We did not apply an ARMA (autoregressive-moving-average model), because the noise inputs of the moving average model were not known before the application of Equation 1 and must be averaged (Kantz and Schreiber, 2004; Costa et al., 2012b).

3.2 Gap-filling streamflow data

We used the outcomes of the Soil Moisture Accounting Procedure (SMAP; Kwon et al., 2012), a

rainfall-runoff model (Lopes et al., 1981) to fill up the gaps of the streamgauges and to increase their available streamflow data. The SMAP Model was set up and calibrated, producing a good performance for the monthly semiarid streamflow at IS and SS with a Nash-Sutcliffe coefficient of 0.78 and 0.86, respectively.

We performed a model calibration under parameter uncertainty for 28 streamgauges, including the IS and SS, using the differential evolution adaptive metropolis (DREAM) algorithm (Vrugt et al., 2008; Vrugt et. al., 2009; Vrugt, 2016). In this study, we considered only the average over the simulated streamflow envelope, which was based on one thousand parameter vectors. They assumed a third of the available data for validation in each streamgauge (following the Split-Sample Test; Klemeš, 1986). Wet, normal and dry years were well represented in both calibration and validation selected periods of the streamgauages, even if this selection varied from one to another. In the case of the IS (SS), the validation data was the streamflow measured from 1944 to 1976 (from 1993 to 2007), while the remaining data from 1912 to 2017 (from 1973 to 2017) was used for model calibration.

3.3 Time series model adjustment and assessment

A cross-validation approach was adopted to evaluate streamflow forecasting. First, to facilitate the comparison of the model results between the studied basins, we had to choose the same validation period for both IS and SS. Second, the streamflow gaps, which were filled up with the rainfall-runoff modelling outputs, had to be concentrated in the training sets. Following these rules, three different intervals from the whole streamflow time series (1951–2015) were chosen for the training set and also for the validation set. The validation (training) sets had to show a good balance between dry, regular and wet streamflow seasons, because interannual variability of semi-arid streamflow is very high (Güntner and Bronstert, 2004). Moreover, it is recurrent dry and wet decades in the Brazilian semi-arid area. Therefore, we selected the period combinations for training and validation sets as shown in Table 1.

Table 1 Period combinations for training and validation sets, which were used for the applied cross-validation approach, given 65-a (1951–2015) streamflow time series at both IS and SS

Combination	Training set	Validation set
I	1951–1979; 1990–2015	1980–1989
II	1951–1989; 2000–2015	1990–1999
III	1951–1999; 2010–2015	2000–2009

The model performance was calculated for each training set and over all validation sets together (30 a in total). There was only one gap in the validation set for both streamgauges, while the remaining gaps, which were filled up with the rainfall-runoff modelling outputs, were concentrated in the training sets. This cross-validation approach is similar to the classical k-folds cross-validation technique, but restricted to a validation period (1980–2009), whose data showed almost no gaps for both streamgauges. Considering that the length of the streamflow time series is short (only 65 a) and much of them were actually the outputs of a rainfall-runoff model, we believe there is a good balance between the length of the validation set and the length of the training set.

LC needed no model adjustment, whereas for LA we adopted the measurements at 2 last steps, which gave the highest correlations with the predictand in the training set (not shown). We tried from 1 to 7 nearest neighbours for k-NN and adjusted the power parameter for all k-NN models that maximize the model performance over the training sets. Application of k-NN models for streamflow time series can be found in many literature (Wu et al., 2009; Wu and Chau, 2010; Tongal, 2020). AR was fitted after the method of least squares for each training set (I, II and III in Table 1). Then, each fitted AR model was used for each validation subset (10 a), respectively.

We assumed that the criterion of acceptance (reliability) of the validation results is the model forecast more skillful than the streamflow climatology. The climatology as a benchmark is adequate, since water management in the studied basins is typically relying on it instead of seasonal

forecasting as a basis for decision making, which was also assumed by Seibert et al. (2017). The RMSE is the standard deviation (SD) of the residuals (forecast errors). So, a higher (lower) RMSE means a lower (higer) model performance. To facilitate the comparison of forecast reliability between the models and the streamflow climatology, we used the standardized root mean square error (SRMSE) as the performance criterion. SRMSE is defined as RMSE divided by the SD of the test set (Perreti et al., 2013). SRMSE greater than unity indicates predictions less accurate than simply predicting the mean of the test set (Perreti et al., 2013). In this study, we defined the mean of the test set (training or validation) as streamflow climatology. So, according to Yossef et al. (2013), when SRMSE is equal to 1.00, the forecast skill is equal to that of a climatological forecast. SRMSE smaller than 1.00 indicates that it is more skillful than climatology; whereas SRMSE greater than 1.00 indicates less skill than climatology. SRMSE approaches 0.00 for a perfect forecast.

For the assessment of the deterministic forecasting of the streamflow, the error was simply calculated applying Equation 1 for training and validation sets. Considering the probabilistic streamflow forecasting, in which we assigned a PDF with a confidence interval for the forecast using the model errors in the training set, the forecast errors in the validation set (ε_v) were calculated in a different manner (Eq. 2).

$$\varepsilon_v = \begin{cases} x_{t+m\Delta t} - F + \xi^+, & \text{if } x_{t+m\Delta t} > F + \xi^+ \\ x_{t+m\Delta t} - F + \xi^-, & \text{if } x_{t+m\Delta t} < F + \xi^- \\ 0, & \text{otherwise} \end{cases}, \tag{2}$$

where ξ^+ (ξ^-) is the upper (lower) limit of the confidence interval and F is the deterministic term. So, when a measurement in the validation set occurred inside the limits of the confidence intervals of the forecast PDF, the error was zero. These errors of Equation 2 are less than those from the application of the deterministic term alone. However, if the length of the chosen confidence interval is too large, the probabilistic forecast may not be useful for real-world issues, even providing a very low SRMSE. Therefore, in the context of probabilistic forecasting, a compromise must be given between the length of the confidence interval and the result SRMSE. In this work, we compared the length of the confidence interval to the SD of the streamflow series. The necessary box-and-whisker plots were generated using the web-tool BoxPlotR (http://shiny.chemgrid.org/boxplotr/).

3.4 Jaguaribe River Basin application

The Jaguaribe River flows normally from January to June at IS and SS. Rarely, river flows are relevant in December and July next year. Since past streamflow measurements are necessary for this approach, we chose the streamflow in March, April, May and June (the middle and end of the rainy season) as predicands at seasonal and monthly scale. We adopted four different lead times: one month ahead for monthly scale and two, three and four months ahead for seasonal scale.

The streamflows in January and February (the beginning of the rainy season) were always predictors at monthly and seasonal scale. However, the number of predictors increases depending on the lead time and the predicand at monthly scale (Table 2). Table 2 shows the 7 forecasts run in this study after the combination of predicands, predictors and lead times. The predicands and predictors in Table 2 are indicated by the month, in which the streamflow is observed. So, we run a monthly streamflow forecasting with a fixed lead time of one month and a variable number of predicands. We also run a SSF with a variable lead time (two, three and four months) and a fixed number of predictors, which were the streamflows in January and February. The streamflow forecasting began (finished) with the predicand in March (June). Although streamflows, which are observed in January and February, show smaller variances (Figs. 2 and 3), they should be taken into account as predictors, because they demonstrated a relevant prediction power at both scales.

An additional difficulty is the dryness at the beginning of the rainy season, because non-flow states in January and February clearly hamper the streamflow forecasting for the remaining season from March to June, using the aforementioned time series models. Therefore, in the case of non-flow states for the predictors, we added a new assumption for the k-NN approach: the nearest

neighbours to the predicand were those also closer in time (the hydrologic persistence; Koutsoyiannis, 2005), besides the Euclidean distance of the traditional k-NN approach.

The construction of reservoirs, land use changes and irrigation schemes, which interact with each other in the study catchments, over the last century may hamper the streamflow predictability. However, there are no shift terms or clear trends in the streamflow time series, which are expected when such nonstationarities are relevant. Therefore, we consider them of minor importance at such a large spatial scale, when compared to data uncertainty and natural streamflow variability, which are quite high for dryland rivers. This assumption allows a priori the applicability of the presented methodology.

Table 2 Developed streamflow forecasting in the Jaguaribe River Basin after the combination of predicands, predictors and lead times.

Predicand	Predictor			
March	Jan, Feb	-	-	-
April	Jan, Feb, Mar	Jan, Feb	-	-
May	Jan, Feb, Mar, Apr	-	Jan, Feb	-
June	Jan, Feb, Mar, Apr, May	-	-	Jan, Feb
Lead time (month)	1	2	3	4

Note: The predicands and predictors are indicated by the month, in which the streamflow is observed. -, not applicable.

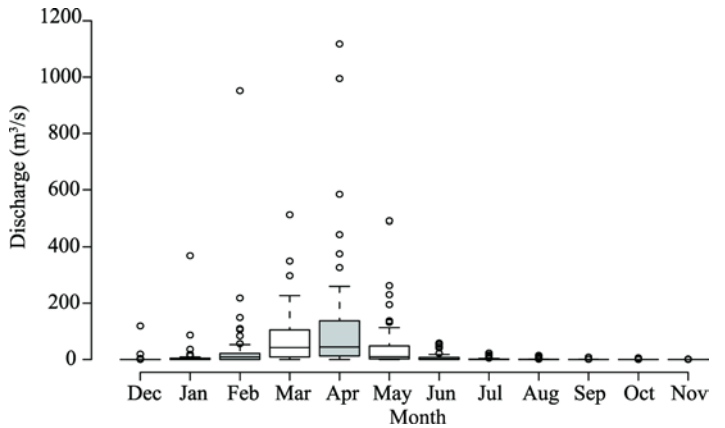

Fig. 2 Average monthly hydrograph (1951–2015) of the Iguatu streamgauge (IS), with 3.7% of gap-filled streamflow data (29 months) using a rainfall-runoff model

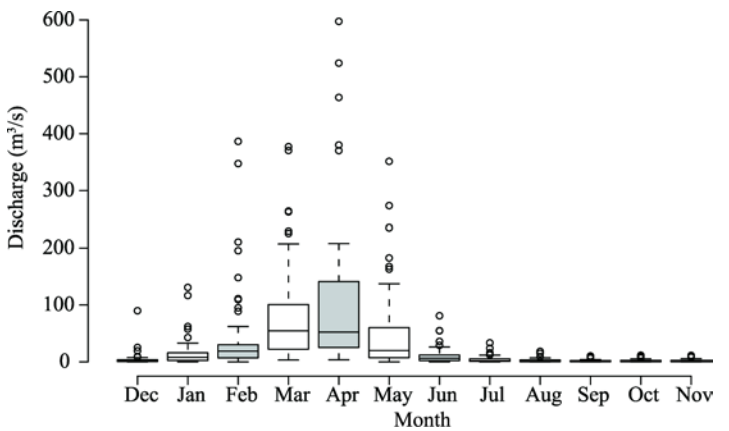

Fig. 3 Average monthly hydrograph (1951–2015) of the Salgado streamgauge (SS), with 35.1% of gap-filled streamflow data (278 months) using a rainfall-runoff model

4 Results

4.1 Gap-filled hydrographs

The average monthly hydrographs of the IS and SS are presented in Figures 2 and 3, respectively, which showed that the high streamflow season occurred only in March, April and May, while negligible river discharge was observed from July to December, except for some discharge outliers at the IS in December and at SS in December and July next year. There were two periods of transition between high and very low streamflow states: the beginning and the end of the streamflow season, which happened in January and February, and in June, respectively. The streamflow in the beginning of the streamflow season was larger than that in the end of the streamflow season.

The rising hydrograph limb took four months from January to April, when the streamflow peak occurred, while the falling limb took just two months (May and June). The streamflow in March prior to the peak was higher than that in May after the peak. In the rising limb, the faster streamflow change happened from February to March, i.e., during the transition between the beginning of the season and the high streamflow season. In the falling limb, the faster change occurred from April (peak flow) to May.

During the high streamflow season, we found the larger streamflows took place in IS, when compared to the streamflows in SS. The beginning and the end of the streamflow season were relatively drier in IS. In the beginning (end) of the streamflow season, we observed a non-flow state in 16 (20) out of 65 a at the IS, whereas the non-flow state in the beginning (end) of the streamflow season happened only once (four times) at the SS. So, the hydrograph was sharper for IS and, for both streamgauges, the end of the season was drier than the other seasons.

4.2 Monthly streamflow forecasting

4.2.1 Deterministic forecasting

The performance of the time series models (k-NN, LC, LA and AR) for each predicand in the validation set is presented in Figure 4. We excluded some outliers, with SRMSE (forecast error) greater than 2.00. Then, we did not show one outlier (AR) for March and April at IS and two outliers (LC and LA) for June at both streamgauges.

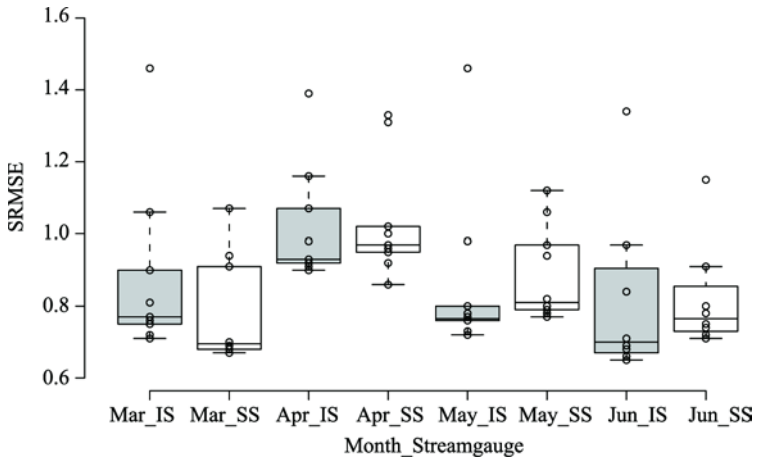

Fig. 4 SRMSE (standardized root mean square error) of the applied time series models in the validation set (1980–2010) for the monthly streamflow forecasting at the IS and SS

Most of the models (73%) performed better than the mean prediction (streamflow climatology), because they showed SRMSE less than 1.00. Their mean SRMSE was 0.80, which was 20% better than the climatology. All months for both streamgauges had at least six models, whose forecast was better than the mean prediction. The models, which showed all SRMSEs less than 1.00, were 3-NN, 4-NN, 6-NN and 7-NN. The 2-NN and 5-NN models showed just one SRMSE value higher

than 1.00. AR had the worst performance with 6 out of the 8 SRMSEs higher than 1.00, followed by LC (5) (LC had 5 out of 8 SRMSEs higher than 1.00) and LA (4) (LA had 4 out of 8 SRMSEs higher than 1.00), respectively.

Considering the best-fit model of each month in the validation set (Table 3), 7 out of the 8 models were a kind of k-NN approach. Only the streamflow in April (peak flow) at IS was better forecast with the LC model, the simplest approach. According to Table 3, SRMSE varied from 0.65 in June (35% better than the mean prediction) to 0.90 in April (10% better than the climatology) at IS. For SS, the SRMSE varied from 0.67 in March (33% better than the mean prediction) to 0.86 in April (14% better than climatology).

Table 3 SRMSE (standardized root mean square error) of the best-fit models in the validation set for the monthly streamflow forecasting at the Iguatu streamgauge (IS) and Salgado streamgauge (SS)

Model performance	Mar_IS	Mar_SS	Apr_IS	Apr_SS	May_IS	May_SS	Jun_IS	Jun_SS
Best-fit model	3-NN	4-NN	7-NN	LC	2-NN	2-NN	5-NN	7-NN
SRMSE Validation	0.71	0.67	0.90	0.86	0.72	0.77	0.65	0.71
SRMSE Training	0.93	0.72	0.89	0.76	0.89	0.80	0.73	0.83

Note: LC, locally constant approach; k-NN, k-nearest-neighbours algorithm with k ranging from 1 to 7. SRMSE is the RMSE (root mean square error) divided by the SD (standard deviation) of the test set (validation or training).

In the rising limb (March and April), the SRMSE in March was less than that in April, when SRMSE was also at the highest, for both streamgauges (Fig. 4). In the falling limb (May and June), a higher SRMSE in May was also the case for both streamgauges. In the high streamflow season (March, April and May), the streamflow was better forecast in March at SS and slightly better in May at IS. Considering the best-fit model of each month in the validation set (Fig. 4; Table 3), we found out the SRMSE in the rising limb at IS was higher than that at SS. However, SRMSE in the falling limb at IS was less than that at SS.

Comparing SRMSE between validation and training sets (Table 3), it was approximately the same for 3 out of the 8 predicands (absolute difference less than 0.03) and higher in the validation set for one predicand (the streamflow in April at SS). However, half of the predicands showed a higher SRMSE in the training set, which were found out for the streamflow forecast in March and June at the both streamgauges.

To illustrate the deterministic streamflow forecasting at monthly scale, we present the forecasts of the best-fit time series model (4-NN) in March at SS (Fig. 5). In the validation set, the model

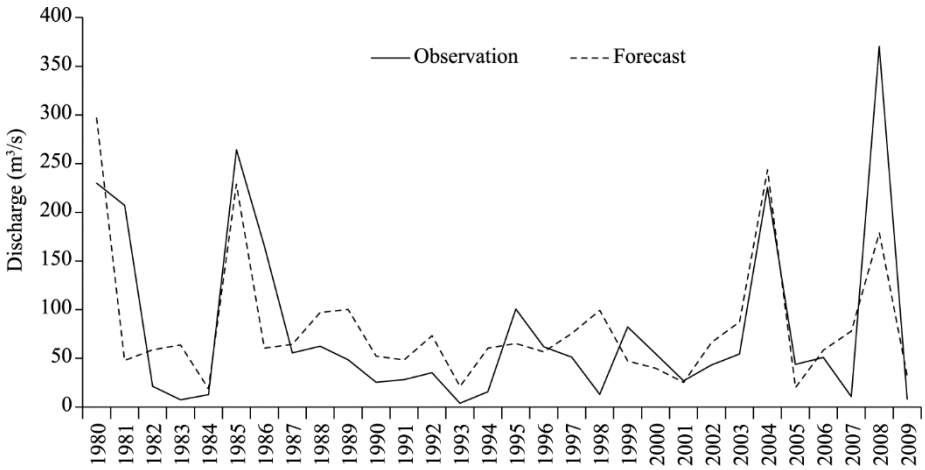

Fig. 5 Monthly deterministic forecasting in the validation set. The predicand is the streamflow in March at the SS. The predictors are the streamflow in January and February. The time series model, which is the best-fit one, is 4-NN. SRMSE (forecast error) in the validation set is 0.67, which means the 4-NN model is 33% better than the mean predictor (climatology). Here, SRMSE is the rms error divided by the SD (standard deviation) of the validation set.

was able to represent well the high, near-average and low flow states, but underestimated the largest peak. Also, the transition between these states (interannual variability) was well simulated, but with some delay in the first decade (1980–1989) of the test set. Overall, the dominant periods of high and low flows were very well differentiated, especially the latter ones.

4.2.2 Probabilistic forecasting

The best-fit time series models (Table 3) were assumed as dynamical parts of Equation 1. Then, we were able to calculate the stochastic term, using the errors in the training set. Table 4a and b show a summary of the forecast PDFs (probability density functions) for each predicand (streamflow in March, April, May and June) at both streamgauges, providing the length of the adopted confidence intervals (33%, 50% and 66%, respectively), SRMSE and the SD of the gap-filled streamflow data.

Table 4a Monthly probabilistic forecasting of the validation set at the IS

Confidence interval	March (92)*		April (204)*		May (79)*		June (12)*	
	Length	SRMSE	Length	SRMSE	Length	SRMSE	Length	SRMSE
33%	39	0.54	49	0.88	12	0.70	2	0.62
50%	72	0.43	93	0.84	31	0.66	3	0.59
66%	128	0.26	195	0.78	55	0.62	6	0.53

Note: The deterministic term of the probabilistic forecasting is based on the best-fit time series model in the validation set and the stochastic term is based on the errors in the training set. *, the numbers in the brackets are the SD (m^3/s) of the gap-filled streamflow series.

Table 4b Monthly probabilistic forecasting of the validation set at the SS

Confidence interval	March (85)*		April (123)*		May (68)*		June (14)*	
	Length	SRMSE	Length	SRMSE	Length	SRMSE	Length	SRMSE
33%	26	0.58	32	0.78	12	0.73	4	0.66
50%	60	0.47	58	0.72	31	0.68	7	0.64
66%	89	0.40	101	0.67	63	0.60	13	0.59

Considering a narrow uncertainty envelope over the deterministic forecasting, i.e., a length of the confidence interval (33%) that was smaller than SD of the streamflow data, the forecasting performance improved expressively for all predicands at SS and for the streamflow in March at IS. Comparing Table 3 and Table 4a and b, SRMSE was reduced by 0.11, 0.08, 0.04 and 0.05 for the streamflow in March, April, May and June at SS, respectively. The highest reduction of SRMSE (0.17) was found for the streamflow in March at IS. The probabilistic forecasting at the narrowest uncertainty envelope (Table 4a and b) outperformed the mean predictor (streamflow climatology) as 46%, 42%, 22%, 27% and 34% for the streamflow in March (IS), March (SS), April (Salgado), May (SS) and June (SS), respectively.

For the other predicands at IS (streamflow in April, May and June), the improvement in the forecasting performance was marginal with a SRMSE reduction of 0.02. Only a wider uncertainty envelope (50% or 66% of confidence interval) led to a better forecasting performance for these predicands. For the streamflow in June, a 66% confidence interval of the in-training-set error distribution, which corresponded to a length of 6 m^3/s (or 50% of streamflow data SD), produced a significant SRMSE reduction of 0.12 with the probabilistic forecasting performing 47% better than the climatology. The same level of SRMSE reduction for the streamflow in April (0.12) and May (0.10) was also achieved at 66% of confidence interval, but showing a much larger length, 96% and 70% of SD for the streamflow in April and May, respectively. The IS probabilistic forecasting for the streamflow in April (May) at the narrowest uncertainty envelope (33%) (Table 4a) outperformed 12% (30%) the mean predictor.

The reason for that slight performance increase even with a larger length of the confidence

interval was mainly two underestimated peaks for the streamflow in April and May. These peaks occurred in 1985 and 1989, which were very moist years. To illustrate the probabilistic forecasting at monthly scale, highlighting the aforementioned difficulty as well, we present the forecasts of the best-fit time series model (2-NN) enveloped by a PDF based on 50% confidence interval of the in-training-set error distribution (Fig. 6). The predicand was the streamflow in May at IS. In the validation set, most of the streamflow data was close to or inside the bounds of the forecast envelope. Although the states of the flows (high, near-average and low) were very well represented, the very high flows in 1985 and 1989 were considerably underestimated. Moreover, there was a relevant overestimation in 1981. As shown in Figure 5, the forecasting in the first decade (1980–1989) of the test set was less reliable compared to the other two decades.

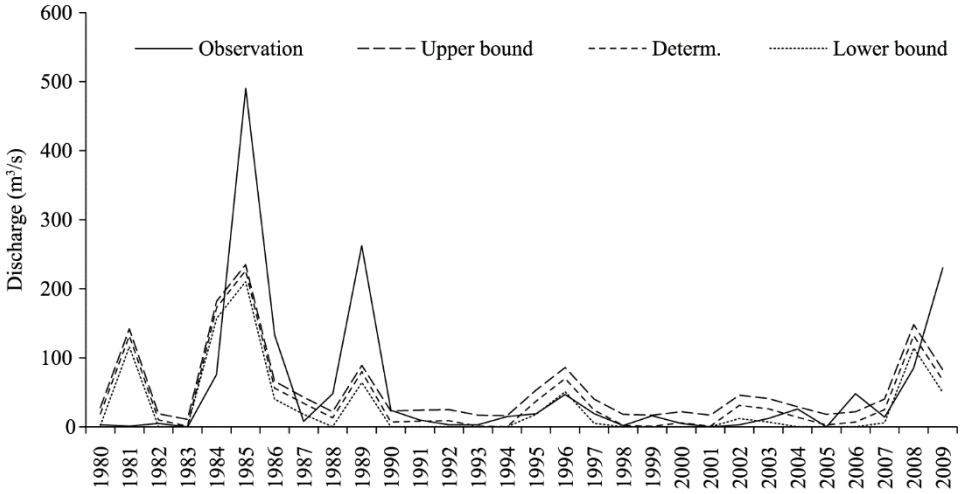

Fig. 6 Monthly probabilistic forecasting in the validation set (30 a) with a confidence interval of 50%, which defines the upper and lower bound forecast. The predicand is the streamflow in May at the IS. The predictors are the streamflow in January, February, March and April. The time series model is 2-NN. SRMSE in the validation set is 0.66, which means the stochastic approach is comparatively 34% better than the mean predictor (climatology).

4.3 SSF

4.3.1 Deterministic forecasting

The performance of the time series models (k-NN, LC, LA and AR) for each predicand in the validation set is presented in Figure 7. We excluded some outliers, whose SRMSE was higher than

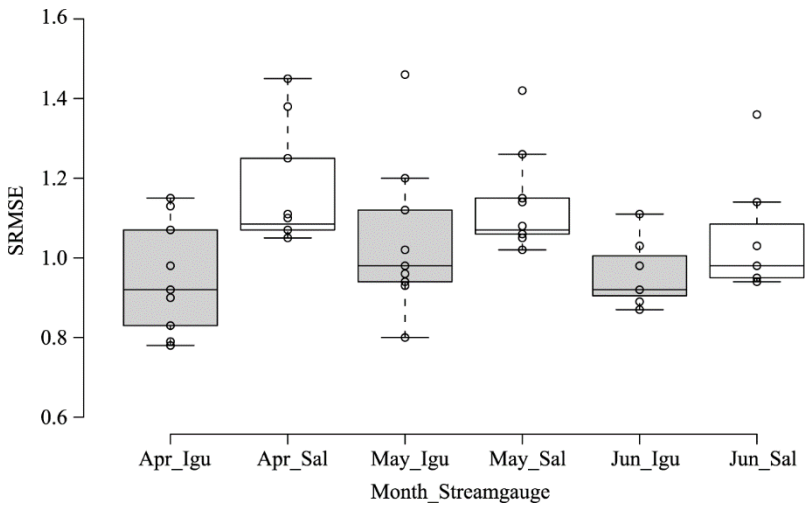

Fig. 7 SRMSE of the applied time series models in the validation set (1980–2010) for the seasonal streamflow forecasting (SSF) in April (Apr), May and June (Jun) at the IS and SS

2.00. Then, we did not show one outlier (AR) for April and May at IS and three outliers (LC, LA and AR) for June at both streamgauges. Note that the SSF in March is not shown, because it is the same as the monthly streamflow forecasting, since the predictors (January and February) are the same.

Most of the models (55%) did not perform better than the mean prediction (streamflow climatology), because they showed SRMSE higher than 1.00. The streamflow forecasting in April and May at SS did not present any time series model, whose forecast was better than the mean prediction. However, for the remaining predicands, there were at least 4 models that showed SRMSEs less than 1.00. The 4-NN, 5-NN, 6-NN and 7-NN models had the best performance with 6 out of the 8 SRMSEs less than 1.00. The 3-NN model showed four SRMSE values less than 1.00. AR had the worst performance with the all SRMSEs higher than 1.00, followed by LA, LC, 1-NN and 2-NN with 6 out of the 8 SRMSEs higher than 1.00.

Considering the best-fit model of each month in the validation set (Table 5), almost all models were a kind of k-NN approach. Only the streamflow in May at IS was better forecast with the LA model. According to Table 5, SRMSE varied from 0.78 in April (22% better than the mean prediction) to 0.87 in June (13% better than the climatology) at IS. For SS, the SRMSEvaried from 0.94 in June (only 6% better than the mean prediction) to 1.06 in May (6% worse than climatology). As expected, the performance of the SSF decreased with the increasing of the lead time at IS: March (SRMSE, 0.71), April (SRMSE, 0.78), May (SRMSE, 0.80) and June (SRMSE, 0.87). SSF performance showed a different behaviour with the increasing of the lead time at SS: March (0.67), April (1.05), May (1.06) and June (0.94). Besides the streamflow in March, the seasonal predicands were better forecast for IS.

Table 5 SRMSE of the best-fit models in the validation set for the seasonal streamflow forecasting (SSF) in April, May and June at the IS and SS

Model performance	Apr_IS	Apr_SS	May_IS	May_SS	Jun_IS	Jun_SS
Best-fit model	6-NN	7-NN	LA	7-NN	7-NN	6-NN
SRMSE validation	0.78	1.05	0.80	1.06	0.87	0.94
SRMSE trainning	0.95	1.03	1.60	1.03	1.04	1.00

Note: SSF in March is not shown, because it is the same as the monthly streamflow forecasting, since the predictors (January and February) are the same.

Comparing SRMSE between validation and training sets (Table 5), it was slightly the same for 2 out of the 6 predicands (absolute difference less than 0.03), which were found out for the streamflow forecast in April and May at SS. The remaining predicands showed a higher SRMSE in the training set.

To illustrate the deterministic streamflow forecasting at seasonal scale, we present the forecasts of the best-fit time series model (6-NN) in April at IS as example (Fig. 8). In the validation set, the model clearly overestimated the streamflow from 1990 to the middle of 2000s and underestimated it in the beginning of 1980s and the end of 2000s. Although over- and underestimating, the model was capable to differentiate well the long periods of high and low flows, including a very well simulation of the largest peak.

4.3.2 Probabilistic forecasting

The best-fit time series models (Table 5) were assumed as dynamical parts of Equation 1. Then, we were able to calculate the stochastic term, using the errors in the training set. Table 6a and b show a summary of the forecast PDFs for each predicand (streamflow in April, May and June) at both streamgauges, providing the length of the adopted confidence intervals (33%, 50% and 66%), SRMSE and the SD of the gap-filled streamflow data. Note that the SSF in March is not shown, because it is the same as the monthly streamflow forecasting, since the predictors (January and February) are the same.

Considering a narrow uncertainty envelope over the deterministic forecasting, i.e., a length of

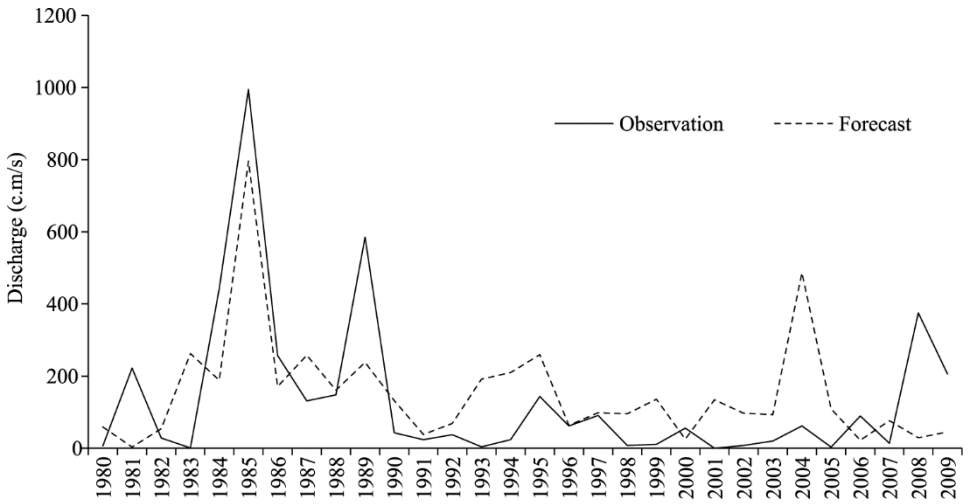

Fig. 8 Seasonal deterministic forecasting in the validation set (30 a). The predicand is the streamflow in April at the IS. The predictors are the streamflow in January and February. The time series model, which is the best-fit one, is 6-NN. SRMSE in the validation set is 0.78, which means the 6-NN model is 22% better than the mean predictor (climatology).

Table 6a Seasonal probabilistic forecasting of the validation set at the IS

Confidence interval	April (204)*		May (79)*		June (12)*	
	Length	SRMSE	Length	SRMSE	Length	SRMSE
33%	81	0.67	40	0.56	5	0.78
50%	139	0.60	73	0.46	10	0.71
66%	235	0.48	98	0.38	16	0.60

Note: The deterministic term of the probabilistic forecasting is based on the best-fit time series model in the validation set and the stochastic term is based on the errors in the training set. SSF in March is not shown, because it is the same as the monthly streamflow forecasting, since the predictors (January and February) are the same. *, the numbers in the brackets are the SD (m^3/s) of the gap-filled streamflow series.

Table 6b Seasonal probabilistic forecasting of the validation set at the SS

Confidence interval	April (123)*		May (68)*		June (14)*	
	Length	SRMSE	Length	SRMSE	Length	SRMSE
33%	54	0.95	24	0.93	5	0.86
50%	110	0.80	37	0.89	11	0.78
66%	164	0.67	58	0.83	18	0.71

the confidence interval (33%) that was smaller than SD of the streamflow data, the forecasting performance improved expressively for all predicands at both streamgauges. Comparing Table 5 to Tables 6a and b, SRMSE was reduced by 0.11 (0.10), 0.24 (0.13) and 0.09 (0.08) for the streamflow in April, May and June at IS (SS), respectively. The highest reduction of SRMSE was found for the streamflow in May, followed by those in April and June, respectively. The probabilistic forecasting at the narrowest uncertainty envelope (Table 6a and b) outperformed the mean predictor (climatology) as follow: 5% (33%), 7% (44%) and 14% (22%) for the streamflow in April, May and June at SS (IS), respectively, showing a much better streamflow forecasting at IS.

5 Discussion

The developed data-driven approach outperformed the streamflow climatology (the mean predictor

in the validation set) for all one-month-ahead streamflows monthly streamflows (8 predicands). On average, it was 25% better than the climatology. SSF was also reliable (on average, 20% better than the climatology), failing slightly only for the high flow season (April and May) of the SS (6% worse than the climatology). Considering an uncertainty envelope, which was 50% and 40% of the data SD, the streamflow forecasting performance increased considerably to 37% and 28% better than the climatology at monthly and seasonal scale, respectively. These findings are an advance regarding the past studies on this subject in the Jaguaribe River Basin (Delgado et al., 2018; Pilz et al., 2019), which were not able to perform better than the streamflow forecasting, and are at the same order of magnitude of studies carried out in other drylands, but using a more complex approach (Yossef et al., 2013; Seibert et al., 2017).

The global nonlinear k-NN approach was the best-fit time series model for 12 out of 14 predicands, although the *k* number of nearest neighbours and the power parameter of the inverse distance weighting interpolation were not the same. The LC and LA approach were the best-fit model for the monthly-scale streamflow in April at SS and the seasonal-scale streamflow in May at IS, respectively. The global linear AR model was the worst-fit time series model for both scales. In the Limpopo River Basin in southern Africa, Seibert et al. (2017) found a different result for a multivariate analysis of the hydrological drought forecasting, in which a multiple linear regression showed the best forecast skill compared to artificial neural networks and random forest regression trees, despite their capabilities to represent nonlinear relationships.

The outputs of the rainfall-runoff model to fill up the gaps of the streamflow series were fundamental to a better streamflow forecasting at SS (modelled data were 35.1% of the whole streamflow series), while their impact on the model performance was negligible at IS (modelled data were only 3.7% of the whole streamflow series). Disregarding the modelled data at SS, for example, the SRMSE of the best-fit time series model increased from 0.67 to 0.75, 0.77 to 0.82 and 0.71 to 0.79 for the monthly-scale streamflow in March, May and June, respectively. There was no performance change for the streamflow forecasting in April, because the best-fit model was the LC that did not need any information from the training set, whose concentrated modelled data. This finding may create new opportunities for streamflow forecasting at monthly and seasonal scale in data scarce regions, leading to positive impacts on water allocation and drought management.

SRMSEs were mainly driven by the streamflow intra-seasonality at monthly scale, while they were by the forecast lead time at seasonal scale. In the context of streamflow forecasting, the latter is a recurrent result and was also observed in other studies, which dealt with the role of the antecedent streamflow or the initial conditions for streamflow forecasting (Yossef et al., 2013; Trambauer et al., 2015).

The monthly-scale streamflow forecasting performed better than the seasonal-scale one, besides the streamflow in April at IS. The monthly-scale rising limb was better forecast for SS, while the monthly-scale falling limb for IS. The former may be explained by the hydrograph sharpness at IS, due to the combination of a drier beginning of the streamflow season and a larger high streamflow season. The latter may be a result of a much more complex baseflow behavior at SS, due to the discharge from and the interaction between the different regional aquifers located in the upstream basin of the Salgado River (Machado et al., 2007).

The seasonal-scale streamflow forecasting from April to June was a much better forecast for IS than SS. This outstanding result of the seasonal-scale streamflow forecasting at IS may be explained by the use of the hydrologic persistence assumption (Koutsoyiannis, 2005), which was quite often presented for IS. This assumption worked always when the beginning of the streamflow season (January and February) showed non-flow, which was the case for 12 out of 30 a in the validation set of each seasonal-scale predicand (April, May and June) at IS.

The probabilistic strategy improved significantly the streamflow forecasting at a narrow uncertainty envelope, although a larger envelope length was found at seasonal scale. This strategy had a better performance in the transition between the beginning of the season and the high flow season (March) at monthly scale and in the transition between the high flow season and the end of the season (May) at seasonal scale. Some of the predicands showed higher SRMSEs in the training

set, which may be explained by the concentration of modelled streamflow data in this set and/or a more complex streamflow series of the training set. However, since higher SRMSEs in the training set led to a larger uncertainty envelope length in the validation set, that possible side effect was taken into account for the construction of the probabilistic forecasting, which presented reliable results even at the narrowest uncertainty envelope.

Monthly and seasonal forecasts have a high uncertainty; therefore, it is an important task to convey the skill of the forecast system, and for end users to include uncertainty information in the decision-making process (Seibert et al., 2017). This is achieved by probabilistic streamflow forecasts that may serve as inputs to water resources operation models, which provide the probability of net benefits or losses for each sector of the economy, such as irrigation, industry and fish farming. If the probability of loss is significant, policymakers may want to divert some resources in advance to mitigation procedures, or at least be prepared for a significant emergency intervention (Sittichok et al., 2016). However, deterministic forecasts are still common practice in many water management systems in Brazil.

6 Conclusion

We developed a data-driven approach to forecast dryland streamflows at monthly and seasonal scale, relying only on the streamflow series itself. The deterministic forecasting was evaluated by the application of four different types of time series model (LC, LA, k-NN and AR). The probabilistic forecasting was based on the deterministic forecast enveloped by a PDF from the time series model errors in the training set. The outputs of a conceptual rainfall-runoff model were used to fill up the gaps of the streamgauges and to increase the available streamflow data. To our knowledge, this kind of hydrological model application for dryland streamflow forecasting has not been reported yet. This methodology was applied for two large catchments in the Brazilian semi-arid area.

Our approach outperformed the climatology for most streamflows at monthly and seasonal scale (12 out of 14 predicands), in which the global nonlinear model and the global linear model were the best-fit and worst-fit time series models, respectively. In the probabilistic strategy, the deterministic forecast enveloped by a PDF, which was considerably narrower than the data SD, increased the forecasting performance by about 50% at both scales. The outputs of the rainfall-runoff model to fill up the gaps of the streamflow series played an important role in improving streamflow forecasting.

The developed data-driven approach is mathematical and computationally very simple, demands few resources to accomplish its operational implementation and is applicable to other dryland watersheds. Moreover, since the studied watersheds have characteristics (e.g., large drainage area, short time series with gaps and high streamflow interannual variability) that are similar to those of drylands in need of streamflow forecasting information, we believe that the transfer potentiality of this study is high. The streamflow forecasts may be part of drought forecasting systems and help plan water allocation months in advance. Moreover, the developed strategy can serve as a baseline for more complex streamflow forecast systems.

Acknowledgements

We thank the Brazilian Water Agency and the Water Company of the State of Ceará of Brazil for streamflow and reservoir data availability. The first author thanks the Brazilian National Council for Scientific and Technological Development for the Post-Doc scholarship (155814/2018-4).

References

Araújo J A de A. 1990. Dams in Northeastern Brazil: an experience in the semi-arid region (2nd ed). Fortaleza: DNOCS, 328.

Bennett J C, Wang Q J, Robertson D E, et al. 2017. Assessment of an ensemble seasonal streamflow forecasting system for Australia. Hydrology and Earth System Sciences, 21: 6007–6030.

Block P J, Souza Filho F A, Sun L, et al. 2009. A streamflow forecasting framework using multiple climate and hydrological models. Journal of the American Water Resources Association, 45(4): 828–843.

Collischon W, Tucci C E M, Clarke R T, et al. 2007. Medium-range reservoir inflow predictions based on quantitative precipitation forecasts. Journal of Hydrology, 344(1–2): 112–122.

Costa A C, Bronstert A, de Araújo J C. 2012a. A channel transmission losses model for different dryland rivers. Hydrology and Earth System Sciences, 16(4): 1111–1135.

Costa A C, Bronstert A, Kneis D. 2012b. Probabilistic flood forecasting for a mountainous headwater catchment using a nonparametric stochastic dynamic approach. Hydrological Sciences Journal, 57(1): 10–25.

Costa A C, Foerster S, de Araújo J C, et al. 2013. Analysis of channel transmission losses in a dryland river reach in north-eastern Brazil using streamflow series, groundwater level series and multi-temporal satellite data. Hydrological Processes, 27(7): 1046–1060.

Crochemore L, Ramos M H, Pappenberger F. 2016. Bias correcting precipitation forecasts to improve the skill of seasonal streamflow forecasts. Hydrology and Earth System Sciences, 20(9): 3601–3618.

Delgado J M, Voss S, Bürger G, et al. 2018. Seasonal drought prediction for semiarid northeast Brazil: Verification of six hydro-meteorological forecast products. Hydrology and Earth System Sciences, 22(9): 5041–5056.

Fioreze A P, Bubel A P M, Callou A É P, et al. 2012. The water issue in the Northeast Brasília: Ministry of Science and Technology. [2020-01-24]. http://livroaberto.ibict.br/handle/1/669.

Formiga-Johnsson R M, Kemper K. 2005. Institutional and Policy Analysis of River Basin Management: The Jaguaribe River Basin, Ceará, Brazil. New York: Social Science Research Network, 42.

Frischkorn H, Santiago M F, de Araújo J C. 2003. Water resources of Ceará and Piauí. In: Gaiser T, Krol M, Frischkorn H, et al, Global Change and Regional Impacts. Berlin: Springer-Verlag, 87–94.

FUNCEME (Foundation for Meteorology and Water Resources of the State of Ceará). 2008. Mapping of the surface of the water bodies in Brazil. Fortaleza: FUNCEME, 108.

Güntner A, Bronstert A. 2004. Representation of landscape variability and lateral redistribution processes for large-scale hydrological modelling in semi-arid areas. Journal of Hydrology, 297(1–4): 136–161.

Güntner A, Krol M S, de Araújo J C, et al. 2004. Simple water balance modelling of surface reservoir systems in a large data-scarce semiarid region. Hydrological Sciences Journal, 49(5): 901–918.

Gutierrez A P A, Engle N L, de Nys E, et al. 2014. Drought preparedness in Brazil. Weather and Climate Extremes, 3: 95–106.

Hastenrath S, Heller L. 1977. Dynamics of climatic hazards in northeast Brazil. Quarterly Journal of the Royal Meteorological Society, 103(435): 77–92.

He Z, Wen X, Liu H, et al. 2014. A comparative study of artificial neural network, adaptive neuro fuzzy inference system and support vector machine for forecasting river flow in the semiarid mountain region. Journal of Hydrology, 509: 379–386.

Kalra A, Miller W P, Lamb K W, et al. 2012. Using large-scale climatic patterns for improving long lead time streamflow forecasts for Gunnison and San Juan River Basins. Hydrological Processes, 27(11): 1543–1559.

Kalra A, Li L, Li X, et al. 2013. Improving streamflow forecast lead time using oceanic-atmospheric oscillations for Kaidu River Basin, Xinjiang, China. Journal of Hydrologic Engineering, 18(8): 1031–1040.

Kantz H, Schreiber T. 2004. Nonlinear Time Series Analysis (2nd ed). Cambridge: Cambridge University Press, 388.

Kirchner J W. 2009. Catchments as simple dynamical systems: Catchment characterization, rainfall-runoff modelling, and doing hydrology backward. Water Resources Research, 45(2): 1–34.

Klemeš V. 1986. Operational testing of hydrological simulation models. Hydrological Sciences Journal, 31(1): 13–24.

Koutsoyiannis D. 2005. Hydrologic persistence and the hurst phenomenon. In: Lehr J H, Keely J. The Encyclopedia of Water. New York: John Wiley & Sons, Inc., 27.

Kwon H H, Souza Filho F A, Sun L, et al. 2012. Uncertainty assessment of hydrologic model and climate forecast model in Northern Brazil. Hydrological Processes, 26(25): 3875–3885.

Lopes J C, Braga J B F, Conejo J L. 1981. Hydrological simulation: Applications of a simplified model. In: III Brazilian Symposium for Water Resources. Fortaleza: ABRH, 42–62.

Machado C J F, Santiago M M F, Mendonça L A R, et al. 2007. Hydrogeochemical and flow modeling of aquitard percolation in the cariri valley-northeast Brazil. Aquatic Geochemistry, 13: 187–196.

Mamede G L, Araújo N A M, Schneider C M, et al. 2012. Overspill avalanching in a dense reservoir network. PNAS, 109(19): 7191–7195.

Moradkhani H, Meier M. 2010. Long-lead water supply forecast using large-scale predictors and independent component

analysis. Journal of Hydrology Engineering, 15(10): 744–762.

Moura A D, Shukla J. 1981. On the dynamics of droughts in northeast Brazil: Observations, theory, and numerical experiments with a general circulation model. Journal of the Atmospheric Sciences, 38(12): 2653–2675.

Nobre P, Shukla J. 1996. Variations of sea surface temperature, wind stress, and rainfall over the tropical Atlantic and South America. Journal of Climate, 9(10): 2464–2479.

Nunes C M. 2012. Project of integration of the San Francisco River with the watersheds in the Northeast - PISF. In: The water issue in the Northeast. Brasília: Ministry of Science and Technology. [2020-01-24]. http://livroaberto.ibict.br/handle/1/669.

Perreti C, Munch S, Sugihara G. 2013. Model-free forecasting outperforms the correct mechanistic model for simulated and experimental data. PNAS, 110(13): 5253–5257.

Philander S G. 1990. El Niño, La Niña, and the Southern Oscillation. International Geophysics Series (vol. 46), San Diego: Academic Press, 293

Pilz T, Voss S, Vormoor K, et al. 2019. Seasonal drought prediction for semiarid northeast Brazil: what is the added value of a process-based hydrological model? Hydrology and Earth System Sciences, 23: 1951–1971.

Porporato A, Ridolfi L. 2001. Multivariate nonlinear prediction of river flows. Journal of Hydrology, 248(1–4): 109–122.

Rao V B, Hada K. 1990. Characteristics of rainfall over Brazil: annual variations and connections with southern oscillation. Theoretical and Applied Climatology, 42: 81–91.

Robertson D E, Wang Q J. 2012. A Bayesian approach to predictor selection for seasonal streamflow forecasting. Journal of Hydrometeorology, 13(1): 155–171.

Rodrigues R R, Haarsma R J, Campos E J D, et al 2011. The impacts of inter-El Nino variability on the Tropical Atlantic and Northeast Brazil climate. Journal of Climate, 24(13): 3402–3422.

Seibert M, Merz B, Apel H. 2017. Seasonal forecasting of hydrological drought in the Limpopo Basin: a comparison of statistical methods. Hydrology and Earth System Sciences, 21: 1611–1629.

Shukla S, Lettenmaier D P. 2011. Seasonal hydrologic prediction in the United States: understanding the role of initial hydrologic conditions and seasonal climate forecast skill. Hydrology and Earth System Sciences, 15: 3529–3538.

Sittichok K, Gado D A, Seidou O, et al. 2016. Statistical seasonal rainfall and streamflow forecasting for the Sirba watershed, West Africa, using sea-surface temperatures. Hydrological Sciences Journal, 61(5): 805–815.

Sivakumar B, Singh V P. 2012. Hydrologic system complexity and nonlinear dynamic concepts for a catchment classification framework. Hydrology and Earth System Sciences, 16: 4119–4131.

Souza Filho F A, Lall U. 2003. Seasonal to interannual ensemble streamflow forecasts for Ceara, Brazil: Applications of a multivariate, semiparametric algorithm. Water Resources Research, 39(11): 1–13.

SUDENE (Superintendência de Desenvolvimento do Nordeste). 1980. Plan for the integrated utilization of the water resources in Northeastern Brazil. Recife: SUDENE, 712.

Takens F. 1980. Detecting strange attractors in turbulence. In: Rang D, and Young L S. Lecture notes in mathematics. Berlin: Springer, 366–381.

Tongal H. 2020. Comparison of local and global approximators in multivariate chaotic forecasting of daily streamflow. Hydrological Sciences Journal, 65(7): 1129–1144.

Trambauer P, Werner M, Winsemius H C, et al. 2015. Hydrological drought forecasting and skill assessment for the Limpopo River basin, southern Africa. Hydrology and Earth System Sciences, 19: 1695–1711.

Uvo C B, Repelli C A, Zebiak S E, et al. 1998. The relationships between tropical Pacific and Atlantic SST and northeast Brazil monthly precipitation. Journal of Climate, 11(4): 551–562.

Vrugt J A, ter Braak C J F, Clark M P, et al. 2008. Treatment of input uncertainty in hydrologic modeling: Doing hydrology backward with Markov chain Monte Carlo simulation. Water Resources Research, 44(12): 1–15.

Vrugt J A, ter Braak C J F, Diks C G H, et al. 2009. Accelerating Markov chain Monte Carlo simulation by differential evolution with self-adaptive randomized subspace sampling. International Journal of Nonlinear Sciences and Numerical Simulation, 10(3): 273–290.

Vrugt J A. 2016. Markov chain Monte Carlo simulation using the DREAM software package: Theory, concepts, and MATLAB implementation. Environmental Modelling and Software, 75: 273–316.

Werner P C, Gerstengarbe F W. 2003. The climate of Piauí and Ceará. In: Gaiser T, Krol M, Frischkorn H, et al. Global Change and Regional Impacts. Berlin: Springer-Verlag, 81–86.

Wilks D S. 2005. Statistical Methods in the Atmospheric Sciences. Burlington: Academic Press, 704.

Wu C L, Chau K W, Li Y S. 2009. Predicting monthly streamflow using data-driven models coupled with data-preprocessing

techniques. Water Resources Research, 45(8), W08432, doi:10.1029/2007WR006737.

Wu C L, Chau K W. 2010. Data-driven models for monthly streamflow time series prediction. Engineering Applications of Artificial Intelligence, 23(8): 1350–1367.

Yassen Z M, Jaafar O, Deo R C, et al. 2016. Stream-flow forecasting using extreme learning machines: A case study in a semi-arid region in Iraq. Journal of Hydrology, 542: 603–614.

Yossef N C, Winsemius H, Weerts A, et al. 2013. Skill of a global seasonal streamflow forecasting system, relative roles of initial conditions and meteorological forcing. Water Resources Research, 49(8): 4687–4699.

Yuan X. 2016. An experimental seasonal hydrological forecasting system over the Yellow River basin – Part 2: The added value from climate forecast models. Hydrology and Earth System Sciences, 20: 2453–2466.

Yuan X, Ma F, Wang L, et al. 2016a. An experimental seasonal hydrological forecasting system over the Yellow River basin – Part 1: Understanding the role of initial hydrological conditions. Hydrology and Earth System Sciences, 20: 2437–2451.